2016

Plasma-Activated Air Mediates Plasmid DNA Delivery In Vivo

Chelsea M. Edelblute
Old Dominion University

Loree C. Heller
Old Dominion University, lheller@odu.edu

Muhammad A. Malik
Old Dominion University, mmalik@odu.edu

Anna Bulysheva
Old Dominion University, abulyshe@odu.edu

Richard Heller
Old Dominion University, rheller@odu.edu

Original Publication Citation

Edelblute, C. M., Heller, L. C., Malik, M. A., Bulysheva, A., & Heller, R. (2016). Plasma-activated air mediates plasmid DNA delivery *in vivo*. *Molecular Therapy — Methods & Clinical Development, 3*, 16028. doi: 10.1038/mtm.2016.28

Citation: Molecular Therapy — Methods & Clinical Development (2016) **3,** 16028; doi:10.1038/mtm.2016.28
Official journal of the American Society of Gene & Cell Therapy

www.nature.com/mtm

ARTICLE

Plasma-activated air mediates plasmid DNA delivery *in vivo*

Chelsea M Edelblute[1,2], Loree C Heller[1,3], Muhammad A Malik[1], Anna Bulysheva[1] and Richard Heller[1,3]

Plasma-activated air (PAA) provides a noncontact DNA transfer platform. In the current study, PAA was used for the delivery of plasmid DNA in a 3D human skin model, as well as *in vivo*. Delivery of plasmid DNA encoding luciferase to recellularized dermal constructs was enhanced, resulting in a fourfold increase in luciferase expression over 120 hours compared to injection only ($P < 0.05$). Delivery of plasmid DNA encoding green fluorescent protein (GFP) was confirmed in the epidermal layers of the construct. *In vivo* experiments were performed in BALB/c mice, with skin as the delivery target. PAA exposure significantly enhanced luciferase expression levels 460-fold in exposed sites compared to levels obtained from the injection of plasmid DNA alone ($P < 0.001$). Expression levels were enhanced when the plasma reactor was positioned more distant from the injection site. Delivery of plasmid DNA encoding GFP to mouse skin was confirmed by immunostaining, where a 3-minute exposure at a 10 mm distance displayed delivery distribution deep within the dermal layers compared to an exposure at 3 mm where GFP expression was localized within the epidermis. Our findings suggest PAA-mediated delivery warrants further exploration as an alternative approach for DNA transfer for skin targets.

Molecular Therapy — Methods & Clinical Development (2016) **3**, 16028; doi:10.1038/mtm.2016.28; published online 13 April 2016

INTRODUCTION

Plasma is a partially ionized gas generated by high-voltage electrical discharges in atmospheric pressure air. In a thermal plasma, temperature of all the particles are nearly equal and high and there is thermal equilibrium.[1,2] Conversely, nonthermal or cold plasmas are not at thermal equilibrium, and only a small percentage of the total gas molecules are charged. As a result, a minimal amount of heat is generated. Cold plasmas are produced when strong applied electric fields accelerate free electrons supplied from the input gas.[3] Noble gases (*i.e.*, helium or argon[4–6]), nitrogenated or oxygenated mixtures,[7,8] or ambient air[9,10] can be used as the working gas. These systems have shown efficacy in clinical applications[11,12] including bacterial inactivation,[9,10,13–15] dentistry,[16,17] wound healing,[4] blood coagulation,[18] dermatology,[19] providing a significant effect on the order of seconds or minutes. Moreover, the bulk of particles produced from cold plasmas are close to room temperature, making them safe for use on heat-sensitive surfaces, such as living tissue.[20]

Physical methods of DNA transfer, including electrotransfer,[21–26] sonoporation,[27] and pressure-based platforms such as hydrodynamic therapy[28] and mechanical massage[29,30] are well tolerated in living tissues.[31,32] Though effective, physical delivery approaches can be considered invasive. A noncontact apparatus would minimize local discomfort at the exposure site. Cold plasma in the form of a high current version of the sliding discharge can be administered without direct contact, where neither the plasma reactor nor the plasma afterglow touches the target surface.[33–35] Instead, the plasma-activated air (PAA) facilitating transfer disperses on the target site.

Utilizing helium-based plasma for DNA transfer has been reported *in vitro* and *in vivo*.[36,37] The therapeutic aims of these studies included delivery of a DNA vaccine to elicit an antigen-specific humoral immune response,[38] and an antitumoral therapy where plasmid DNA encoding the cytokine IL-28 was delivered.[39] While efficient delivery of plasmid DNA was achieved, alternative types of plasma systems may be advantageous. The device used in the current work operates using ambient air as the input gas for plasma generation. This eliminates the incorporation of an external gas tank, making the footprint for the entire system smaller and more portable.

In the current work, we tested PAA-mediated DNA transfer in a human skin model and an animal model to determine if this platform would deliver plasmid DNA to skin. We previously demonstrated utilizing PAA as a DNA transfer method *in vitro*.[40] Recellularized human dermis was used as a preliminary substrate before progressing to a mouse model. For *in vivo* testing, an animal model using BALB/c mice, a strain typically used for vaccine testing, was employed to determine the potential use of PAA as a noncontact DNA transfer method to a living tissue. Plasmid DNA encoding the reporter genes luciferase and green fluorescent protein (GFP) were used to determine both the kinetics and distribution of PAA-mediated DNA delivery.

RESULTS

Twenty-four hours following a 3-minute PAA exposure, luciferase expression in the recellularized dermal constructs peaked (Figure 1). Average total flux results for a 3-minute exposure were 8.44×10^5 photons/second (p/s) after 72 hours. This was significant compared to an intradermal injection of gWizLuc alone ($P < 0.05$). A significant increase in luciferase expression was also observed 120 hours post-PAA exposure ($P < 0.05$).

[1]Frank Reidy Research Center for Bioelectrics, Old Dominion University, Norfolk, VA, USA; [2]Department of Biology, College of Science, Old Dominion University, Norfolk, VA, USA; [3]School of Medical Diagnostic & Translational Sciences, College of Health Sciences, Old Dominion University, Norfolk, VA, USA. Correspondence: R Heller (rheller@odu.edu)
Received 17 November 2015; accepted 7 March 2016

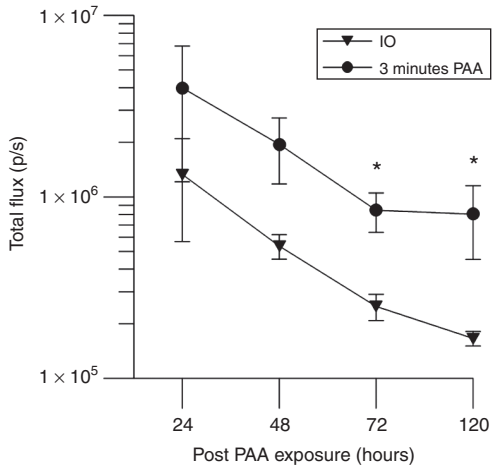

Figure 1 Plasma-activated air (PAA)-mediated gWizLuc delivery in recelullarized dermal constructs. Luciferase expression was monitored in total flux (photons/second) over a 120-hour period following PAA exposure. The experimental condition used was a 3-minute PAA exposure at a 10 mm distance from the injection site. Results were compared to levels achieved from injection only controls. Mean ± standard error of the mean, $n = 3$. *$P < 0.05$.

Table 1 Metabolic activity in recellularized dermis post PAA-exposure

	Time postexposure (hours)		
Group	1	24	48
Injection only	83.75 ± 6.87%	86.13 ± 1.90%	84.02 ± 12.26%
Three-minute PAA	90.44 ± 7.18%	88.97 ± 2.67%	74.47 ± 6.02%

PrestoBlue cell reagent measuring metabolic activity was used for viability analysis. The experimental group is a PAA exposure of 3 minutes after intradermal injection of plasmid DNA. Mean % viability ± standard error of the mean, $n = 3$. Results are not significant with respect to samples receiving only the plasmid DNA injection without PAA exposure.
PAA, plasma-activated air.

Following PAA exposure, metabolic activity did not drop significantly with respect to samples injected with plasmid DNA only at each respective time point (Table 1). Two hours post-PAA exposure, metabolic activity in the injection only control and in samples receiving a 3-minute PAA exposure was similar. Metabolic activity decreased slightly 24 hours after exposure, but this decrease was observed in both experimental and injection only control samples. A similar observation was made 48 hours postexposure. Fluorescence intensity values were significantly higher in samples that did not receive an injection or PAA exposure (data not shown).

Fluorescence images of recellularized dermal constructs receiving PAA exposure following injection of gWizGFP indicate a positive GFP signal was observed on the fluorescein isothiocyanate channel (Figure 2). When these images are merged with corresponding micrographs on the 4′, 6-diamidino-2-phenylindole dihydrochloride channel, it is clear the GFP expression is present in the cytoplasm (Figure 2d–f). Expression is localized within the epidermis. Positive GFP signal above background was not observed in controls receiving only an intradermal injection of gWizGFP without PAA exposure (Figure 2a–c).

Temperature fluctuations in the PAA-exposed mouse skin were negligible (Table 2). Luciferase expression levels in BALB/c mice were higher in the PAA-exposed sites relative to injection only for the entire 4-week follow-up period (Figure 3). Quantitative expression results obtained on day 7 were 9.75×10^6 and 5.47×10^7 p/s for a 3-minute PAA delivery, at a 3 and 10 mm distance respectively. This represents an 82- and 460-fold difference for a 3 mm and 10 mm PAA delivery distance with respect to expression levels obtained from injection only ($P < 0.001$). Peak luciferase expression was achieved 17 days following exposure at a 10 mm distance from the injection site where the average total flux was 5.55×10^7 p/s ($P < 0.05$). Though expression levels tended to be higher in sites receiving PAA at a 10 mm distance, this result was not significant compared to PAA delivered at a 3 mm distance.

Fluorescence images of sectioned mouse skin samples receiving PAA exposure indicate positive GFP signal observed on the TRITC channel after immunostaining (Figure 4). When these images are merged with corresponding micrographs on the 4′, 6-diamidino-2-phenylindole dihydrochloride channel, it is clear that GFP expression is present in the cytoplasm of epithelial cells. PAA exposure at a further distance of 10 mm (Figure 4j–l) appears to enhance GFP expression compared to exposure at a 3 mm distance (Figure 4g–i). Adipocytes in the field of view display auto fluorescence, even in the control receiving no plasmid DNA or PAA exposure, suggesting this is not a positive GFP signal (Figure 4a–c). Expression extends from the epidermal to dermal layers in the samples receiving PAA exposure at a distance of 10 versus 3 mm, suggesting an increased exposure distance delivers the plasmid DNA to cells deeper within the tissue. Positive GFP signal above background was not observed in the injection only control (Figure 4d–f).

DISCUSSION

The current study evaluated PAA-mediated plasmid DNA delivery in a 3D human skin model, as well as *in vivo*. We previously reported the use of PAA for DNA transfer *in vitro*.[40] Initially, recellularized human dermal constructs were employed as an alternative delivery substrate before moving to an animal model. The recellularized dermal constructs provided a 3D structure more akin to human skin, and superior to existing *in vitro* skin models.[41] Three weeks grown at an air-liquid interface provided sufficient time for the epithelial cells to differentiate, allowing for a functional epithelium to form in culture.

Three minutes of PAA exposure enhanced the delivery of gWizLuc to recellularized dermal constructs compared to an injection only control. No significant drop in viability of the constructs as a consequence to PAA exposure was observed. Furthermore, PAA-mediated delivery of gWizGFP to recellularized dermal constructs was confirmed by observing positive GFP expression in the upper epidermal layers and within the base of a hair follicle. No positive signal above background was observed in the injection only control.

An *in vivo* murine model in BALB/c mice was used to test PAA-mediated plasmid DNA transfer to living tissue. We first determined the heat generation from this approach, as a nonthermal platform would be ideal for reducing the damaging effects of excess skin-heating. Temperature measurements were taken at the shorter exposure distance of 3 mm, the closest tested distance from the plasma source, where the generation of heat would likely be highest. No significant changes in temperature at the exposed site following PAA exposure were recorded, suggesting heat does not facilitate DNA transfer in this approach.

Quantitative results measured over 28 days displayed luciferase levels 460-fold greater in PAA-exposed mouse skin sites than levels obtained from the injection of gWizLuc alone. Increasing

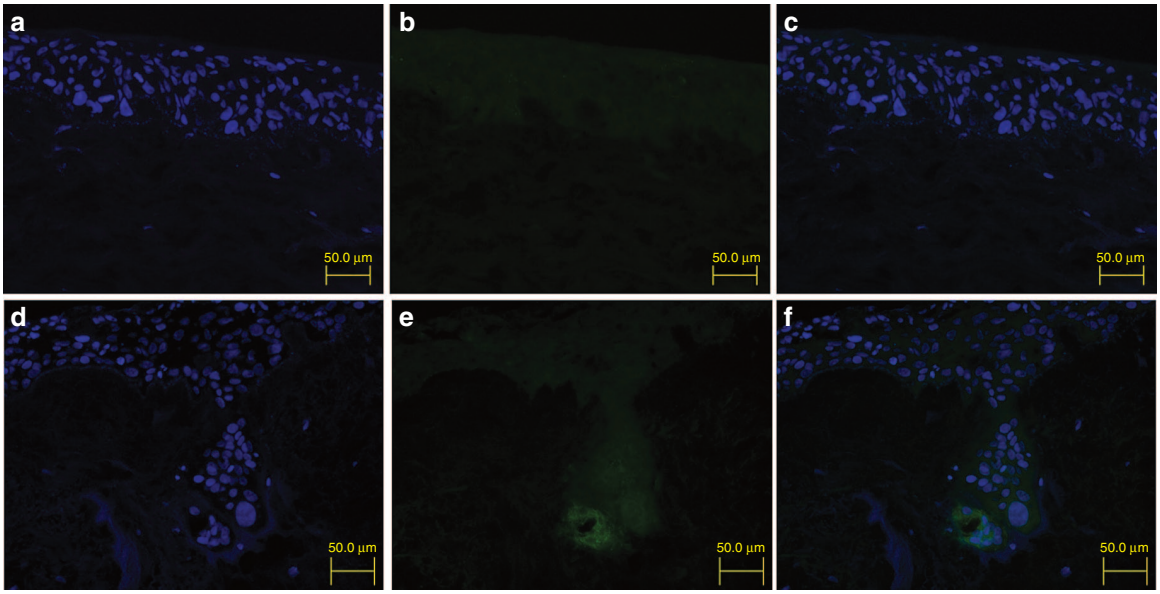

Figure 2 GFP expression in recellularized dermal constructs. An immunostaining protocol using a goat polyclonal anti-GFP antibody fluorescein isothiocyanate (FITC) (ab6662, Abcam, Littleton, CO) as the primary antibody was performed on fixed cryosectioned constructs. 4′, 6-Diamidino-2-phenylindole dihydrochloride (DAPI) nuclear stain was used to determine location of expression. (**a–c**) Intradermal injection of gWizGFP only control on DAPI (left) and FITC (center) channels, overlaid image in right column. (**d–f**) Constructs exposed to PAA for 3 minutes after intradermal injection of gWizGFP. $n = 3$. Scale bar = 50.0 µm. 200×.

Table 2 Skin surface temperature following PAA exposure

Group	*Temperature (°C)*
Before PAA exposure	26.6 ± 0.1
After 3 minutes PAA	26.1 ± 0.6

Surface temperature of the exposed region was measured using an infrared probe. Measurements were taken immediately before and after a 3-minute PAA treatment at a distance of 3 mm. Mean ± standard error of the mean, $n = 4$.
PAA, plasma-activated air.

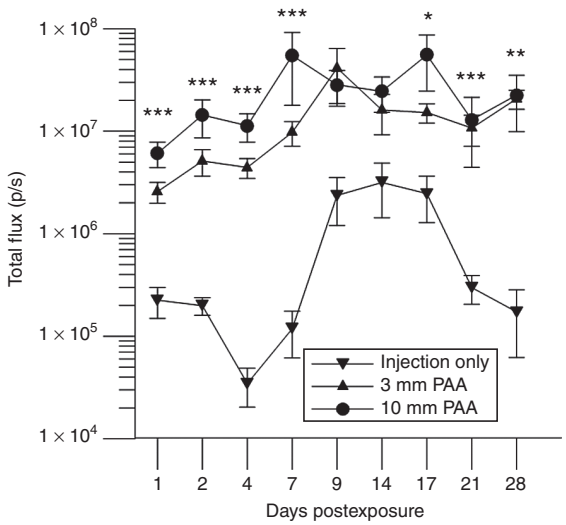

Figure 3 Plasma-activated air (PAA)-mediated gWizLuc delivery in BALB/c mice. Luciferase expression was monitored in total flux (photons/second) over a 28-day period following PAA exposure. Treatment parameters included a 3-minute PAA exposure at either a 3 or 10 mm distance from the intradermal injection site. Results were compared to levels achieved from injection only controls. Mean ± standard error of the mean, $n = 4$ injection only, $n = 8$ per experimental group. *$P < 0.05$; **$P < 0.01$; ***$P < 0.001$.

the distance between the plasma device and the target surface enhanced expression levels. This result further confirms that heat does not facilitate transfer of plasmid DNA in this approach. Gross observation and monitoring of the mice after plasma exposure revealed no apparent levels of discomfort or skin deformations at the delivery site. The animals maintained activity and consumption levels for the entire monitoring period.

PAA-mediated delivery of gWizGFP to mouse skin was confirmed by analyzing GFP expression. Immunostaining of the harvested tissue indicated that delivery of gWizGFP extended beyond the lower epidermis with an exposure at a distance of 10 mm, while GFP expression was localized in the upper epidermis in the group receiving an exposure at the shorter distance of 3 mm.

We previously confirmed the presence of ozone and NO_2 in the plasma-activated gas under operating parameters.[40] It is probable that the generation of diluted reactive species in the PAA assists plasmid DNA delivery. Both ozone and NO_2 effect cellular membranes, and the effects are enhanced with increasing product amounts.[42,43] Viability results suggest the concentrations of these species in the PAA are minimally toxic. The mechanism of PAA-mediated delivery has not yet been elucidated, but it is the consensus that plasma composition alone, *i.e.*, reactive oxygen species and reactive nitrogen species production is not enough to explain plasma-induced effects. Disruption of E-cadherin-based cell junctions and down-regulation of E-cadherin mRNA was reported following nonthermal plasma exposure, leading to a reversible decrease in barrier function.[44] In particular, one group used a nonmetallic electric field probe to measure the electric field at the plasma plume and within plasma targets, showing that an electric field strength up to 1 kV/cm was achieved with the Plasma Gun at a depth up to several millimeters.[45,46] These field strengths suggest electropermeabilization is happening with plasma exposure, and could allow for a plasmid to be driven through transient membrane holes.[36,37]

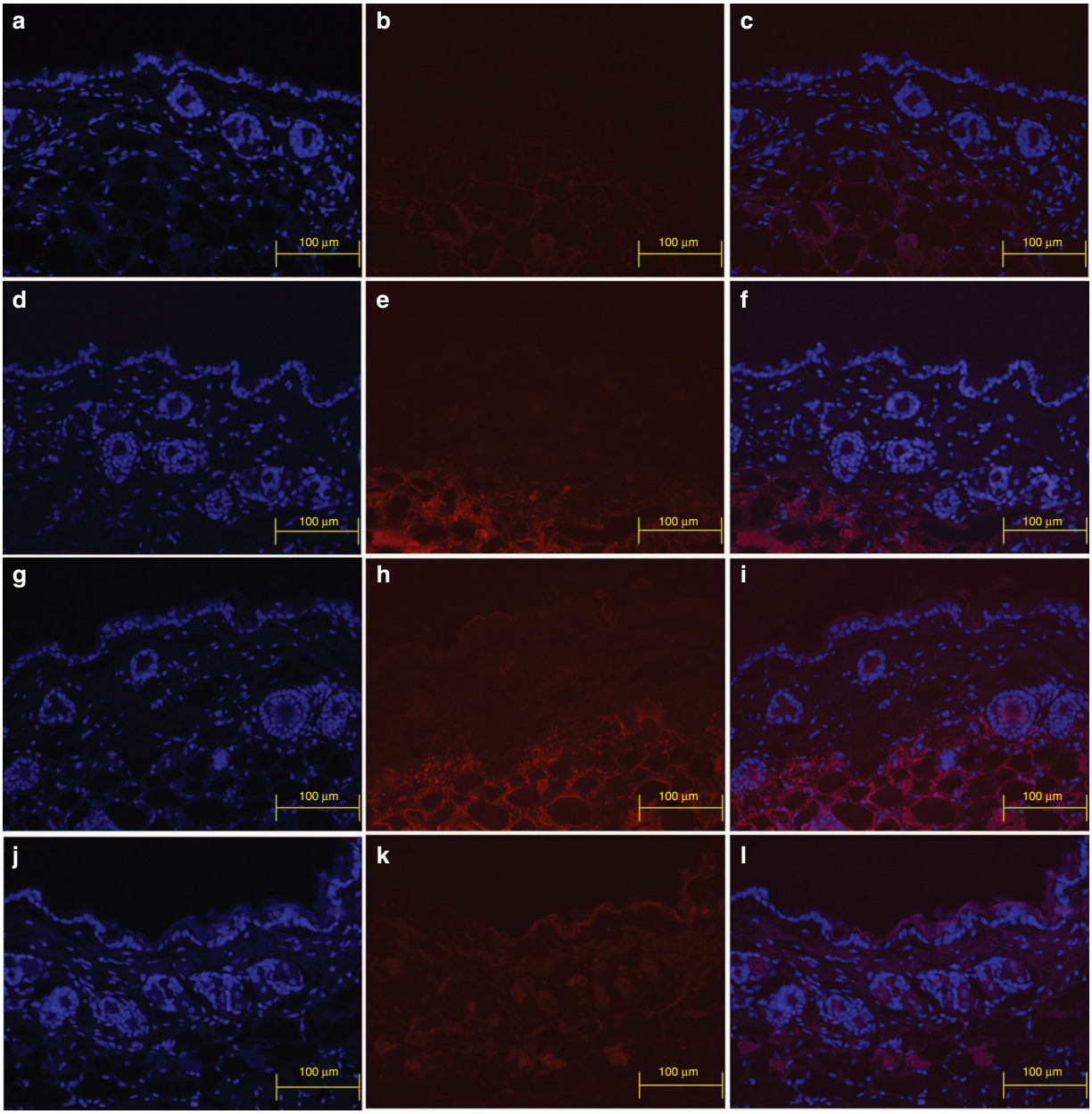

Figure 4 GFP expression in mouse skin biopsies. An indirect staining protocol using a biotinylated anti-GFP primary antibody and secondary antibody, streptavidin eFluor 605 was performed on sections fixed in 4% paraformaldehyde. 4′, 6-diamidino-2-phenylindole dihydrochloride (DAPI) nuclear stain was used to determine expression localization. (**a–c**) sham control without injection of plasmid DNA or plasma-activated air (PAA) exposure on DAPI (left column) and TRITC (center column) fluorescence channels, overlaid image in right column. (**d–f**) injection only control. Three-minute PAA exposure at a distance of 3 mm (**g–i**) and 10 mm (**j–l**). $n = 6$. Scale bar = 100 μm. 200×.

The proposed mechanism in the current approach is electrophysical, *i.e.*, when sufficient electrostatic charge is deposited on the cell membrane it causes outward electrostatic stress that induces electroporation and subsequent entry of plasmid DNA into the cell. Plasma-induced electrostatic stress can be strong enough to rupture the membrane after plasma exposure, *e.g.*, bacterial decontamination,[9,10,13,47] but the lower field strength used in this study avoids this effect. Plasma operating parameters, including the applied voltage, remained constant in this study where only the distance between the plasma reactor and the target site was adjusted. The size of the port where the PAA exits compared to the size of the intradermal plasmid DNA injection is much smaller, suggesting charge dispersal across a relatively larger area would be necessary for transfer. We were able to achieve this by increasing the distance between the plasma reactor and the skin. Based on our results *in vivo*, the increased air flow dispersal permitted by a 10 mm distance versus a 3 mm distance to the target site allows for a more widespread accumulation of electrostatic charge, enhancing plasmid DNA delivery and resulting in higher expression levels and deeper expression distribution within the PAA-exposed tissue.

The novel nonthermal plasma reactor presented provides effective plasmid DNA delivery *in vivo*, with skin as the target tissue. Though a significant increase in expression is achieved, compared to some other DNA transfer methods expression levels are lower. Current nonviral methods have their disadvantages. Direct injection is the most widely used nonviral DNA transfer platform, yet delivery

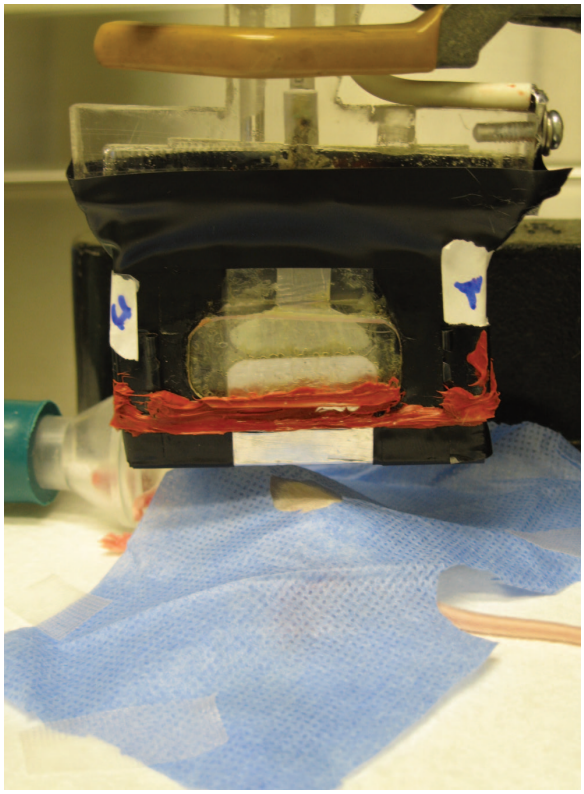

Figure 5 Orientation of plasma reactor *in vivo*. The reactor was placed longitudinally above the site of injection at the respective height of the treatment condition: 3 or 10 mm. This created two equal hemispheres beyond the outer limits of the plasma-activated air (PAA) exit slit. A surgical drape was placed around the site of injection prior to PAA exposure.

levels are poor and expression is localized solely at the site of injection. Sonoporation, using ultrasonic waves to deliver microbubble-contained compounds is limited by proximal organs and bones. Mechanical massage, a noninvasive pressure-based gene delivery approach, yields peak expression 6 hours after the plasmid DNA is introduced. This level drops to baseline soon after, and repeat injections and massage must be administered to achieve the same effect.[29,30] Electrotransfer shows promise for drug and gene therapy, though temporary pain was reported by patients after pulse application. Expression levels achieved with electrotransfer are approximately eightfold higher than what we achieved with PAA in this study.[48–50] However, there was no observable tissue damage from PAA exposure, as is a concern with electrotransfer at higher field strengths. Compared to all of these aforementioned methods, PAA does not require any direct electrode contact with the target to facilitate DNA transfer. We therefore emphasize that PAA would make a good noncontact alternative if multiple treatments are necessary, or to minimize patient discomfort.

This plasma system generating PAA is portable and scalable to accommodate delivery to larger areas.[33] The level of expression achieved with PAA may be advantageous for some therapies where overexpression of the transgene could lead to toxic effects. Our work did not systematically determine parameters needed for controlled expression, a critical aspect for therapeutic development. These studies could augment the potential use of cold plasmas in healthcare settings.

Nonetheless, due to its noncontact application this method would be attractive to both patients and healthcare professionals. Certain cohorts of patients including the young and elderly, or those with diabetes or cancer are more susceptible to infection and other treatment complications, and would assume a lower risk using non-invasive delivery methods. In the future, histological analysis will be necessary to determine the local impact of PAA exposure on tissue. Our results prove PAA can be used to deliver plasmid DNA *in vivo* with skin as the delivery target, providing both the kinetic and distribution expression patterns achieved with this platform at the current operating parameters. PAA-mediated delivery warrants further exploration as an alternative or supplemental DNA transfer approach.

MATERIALS AND METHODS

Plasma system

The reactor has been previously described.[10,33,40] Briefly, it consists of two parallel glass dielectric plates; separated by spacers, with aluminum foil electrodes placed perpendicular to the applied air flow, creating an inter-electrode gap of 2.0 cm in the discharge chamber. Sliding plasma discharges were formed at solid-gas interface along the glass dielectric layer in the discharge chamber measuring 2.6×2.0×0.038 cm. For operating parameters used in this study, the high-voltage electrode was pulsed biased positively by applying a pulsed voltage of 12±0.5 kV peak voltage, 50 ns rise time, 100 ns duration (full width at half maximum) at a repetition rate of 500 Hz. Ambient air supplied at a flow rate of 5 SLM from a Whisper AP 300 fish tank air pump was used as the input gas.

For PAA-mediated plasmid DNA delivery in the animal model, the exit slit of plasma reactor was oriented longitudinally above the injection site, creating two equal hemispheres on either side of the reactor's outer limits (Figure 5). The same set-up position was used for PAA-mediated plasmid DNA delivery to the human skin model.

Plasmids

Endotoxin-free plasmids gWizLuc and gWizGFP were commercially prepared to ensure quality (Aldevron, Fargo, ND) and suspended in sterile injectable saline at 2 mg/ml. For all experiments, 100 µg in a 50 µl volume of respective plasmid DNA was used per experimental or control sample or animal.

Recellularized dermis

The dermal constructs utilized contained three components. DermACELL (LifeNet Health, Virginia Beach, VA) which are decellularized skin grafts, human primary dermal fibroblasts (ATCC, Manassas, VA) and a human Keratinocyte cell line (HaCaT). Fibroblasts were maintained in culture with Dulbecco's Modified Eagle Medium, 10% fetal bovine serum, 1% penicillin/streptomycin at 37 °C and 5% CO_2. HaCaT cells were maintained in culture using both the same media formulations and growth conditions as the fibroblasts. Prior to use, DermaCell grafts were washed in Dulbecco's phosphate-buffered saline and cut into 12 mm disks using a biopsy punch, then washed twice with Dulbecco's Modified Eagle Medium media.

Recellularizing the dermal constructs was performed using a previously developed and validated protocol.[51] Briefly, the procedure is performed in a 12-well plate. DermaCell is placed in the well and then 1×10^6 fibroblasts/disk were placed on the reticular face of the dermis. After one week of growth, 1.5×10^5 HaCaT cells/disk were added to the papillary face of the graft (disk is turned over). Following overnight incubation, the grafts were moved to the upper chamber of Transwell Permeable Supports (Corning Incorporated, Life Sciences, Tewksbury, MA). The bottom well was filled with media, while the top well was left void of media. Recellularized dermis was cultured for 3 weeks with daily media changes before PAA-mediated plasmid DNA delivery.

Viability analysis

PrestoBlue Cell viability assay (Molecular Probes, Carlsbad, CA) was used to measure the metabolic activity of recellularized dermis following PAA exposure. Briefly, the constructs were incubated with the PrestoBlue reagent for two hours, after which 850 µl of each well was transferred in duplicate to a 24-well plate. Fluorescence was recorded by setting excitation and emission at 560 and 590 nm respectively. Duplicate experimental wells were averaged. Control wells containing reagent only were averaged and subtracted as background from the fluorescence value of each experimental well. Measurements were taken 2, 24, and 48 hours postexposure. Percent viability was determined by dividing the fluorescence intensity of samples

injected with plasmid DNA alone and PAA-exposed constructs by controls that were not injected or exposed to PAA at each respective time point.

Animal model

A murine model using BALB/c mice was employed. All procedures were approved by the Old Dominion University Institutional Animal Care and Use Committee. A total of 20 female 8-week-old BALB/c mice of the same age were used for this study. Mice were anesthetized during all deliveries. To anesthesize, animals were placed in an induction chamber infused with a mixture of 3–5% isofluorane and 97% oxygen gas for several minutes. After anesthetized, mice were fitted with a standard rodent mask supplied with 2–3% isofluorane and oxygen to maintain a surgical plane of anesthesia. After exposure, each mouse was monitored continuously until recovered from anesthesia, as indicated by their ability to maintain sternal recumbency and to exhibit purposeful movement.

Temperature measurements

An infrared probe (NationSkander California, Anaheim, CA) was used for recording temperature measurements at the mouse skin surface of each exposed site. The infrared probe was not used while the plasma reactor was in operation. Instead, the temperature was measured immediately before and after application of a 3-minute exposure of PAA at a 3 mm distance.

PAA exposure

Recellularized dermal constructs cultured for 3 weeks were split into three groups. One hundred micrograms of gWiz-LUC was intradermally injected in a volume of 50 µl (2 mg/ml) to the constructs. The experimental group was exposed to 3 minutes of PAA at a distance of 10 mm immediately following injection of plasmid DNA. An injection only control and a control without injection of plasmid DNA were included for comparison.

For the *in vivo* study, each mouse received two experimental sites, one each on opposing flanks. gWizLuc was injected intradermally to shaved flanks in a 50 µl volume (100 µg total, 2 mg/ml) immediately before PAA exposure. The plasma reactor was placed longitudinally above the injection site at a constant distance of either 3 or 10 mm. Operating parameters were set as previously described. An exposure duration of 3 minutes was tested, where the reactor remained stationary during the entire exposure.

Luciferase expression

Luciferase gene expression in the recellularized dermal constructs was measured 24, 48, 72, and 120 hours after PAA exposure. Old media was removed and replaced with fresh media containing 150 µg/ml Luciferin. Samples were incubated in the dark for 5 minutes and then imaged with a Caliper In Vivo Imaging Spectrum whole body imaging system (PerkinElmer, Waltham, MA). Luciferase expression was quantified as total flux measured in photons per second.

Kinetic luciferase expression *in vivo* was monitored over a 28-day period using a Caliper In Vivo Imaging Spectrum whole body imaging system (IVIS). For imaging, the animals were anesthetized in the same manner as described for delivery. Anesthesia was maintained in the imaging chamber by use of an anesthesia block supplying five nose cones. Once the animals were anesthetized, an intraperitoneal injection of 200 µl D-luciferin at a concentration of 15 mg/ml, was given. The mice were imaged 5 minutes after the luciferin injection, representing peak signal detection.

Each mouse received one specific delivery parameter on both of its flanks. In addition, the opposing flank was blocked during PAA exposure using a surgical sheet, allowing for sole exposure of the injection site. Kinetic luciferase expression in BALB/c mice following PAA exposure was measured nine times over a 28-day period. Images were taken on days 1, 2, 4, 7, 9, 14, 17, 21, and 28 post-PAA exposures. A region of interest was drawn around the sites with positive signal. An area of unexposed skin was also measured and subtracted as a background measurement from total flux values. The average of each experimental condition was determined ± standard error of the mean.

GFP expression

Recellularized dermal constructs cultured for 3 weeks were split into three groups. One hundred micrograms of gWiz-GFP was intradermally injected in a volume of 50 µl (2 mg/ml) to the constructs. The experimental group was exposed to 3 minutes of PAA at a distance of 10 mm immediately following injection of plasmid DNA. An injection only control and a control without injection of plasmid DNA were included for comparison.

For the *in vivo* study, each mouse received two experimental sites, one each on opposing flanks. The flanks were shaved prior to injection of plasmid DNA. gWizGFP was injected intradermally in a 50 µl volume (100 µg total, 2 mg/ml) immediately before PAA exposure. A surgical drape was used to prevent exposure of the opposing flank. The plasma reactor was placed longitudinally above the injection site at a constant distance of 10 mm. Exposure distance and duration were chosen per the luciferase expression profile achieved at these parameters. Operating parameters were set as previously described. All exposures were performed in a biosafety cabinet. After PAA exposure, each mouse was monitored continuously until recovered from anesthesia, as indicated by their ability to maintain sternal recumbency and to exhibit purposeful movement.

Animals were humanely euthanized 48 hours after PAA exposure. Sterile skin biopsy punches measuring 12 mm in diameter were used to harvest the tissue at the location where the plasmid DNA was injected. Both the recellularized dermis and the mouse skin punches were fixed in 4% paraformaldehyde at this time point. Fixed samples were transferred to a solution of equal parts Optimal Cutting Temperature compound and 1× Dulbecco's phosphate-buffered saline, and placed on a rotator overnight. The following day, the solution was replaced with 100% Optimal Cutting Temperature compound, and placed back on a rotator overnight. The samples were embedded in Optimal Cutting Temperature compound, frozen at −80 °C, cryosectioned, and mounted to glass slides for staining and observation.

Immunostaining

All washes and staining procedures were performed in the dark to prevent fluorescence bleaching. A 0.05% phosphate-buffered saline with Tween20 stock containing 1× Dulbecco's phosphate-buffered saline and Tween20 was the diluent for all solutions unless otherwise stated. To permeabilize the tissue, each slide was covered with 0.1% TritonX and incubated at room temperature for 20 minutes. The solution was aspirated, and then washed with 0.05% phosphate-buffered saline with Tween20. Sections were blocked in 4% bovine serum albumin for 1 hour. After blocking, a goat polyclonal anti-GFP antibody (fluorescein isothiocyanate conjugated) (ab6662, Abcam, Littleton, CO) was added to each slide in a 200 µl volume at a 1:100 dilution in 4% bovine serum albumin. Sections were incubated in the primary antibody overnight at 4 °C.

Following overnight incubation, the sections were washed in 0.05% phosphate-buffered saline with Tween20 for 5 minutes on a rotator. This washing procedure was repeated four times for a total of five washes. The nuclear dye 4′, 6-diamidino-2-phenylindole dihydrochloride was added at a 1:200 dilution to each slide to determine localization of expression. After 5 minutes, grafts were washed once and coverslips were mounted with VECTASHIELD HardSet mounting medium (Vector Laboratories, Burlingame, CA). The samples were stored at −20 °C until imaging.

Immunofluorescence micrographs were taken on an Olympus IX71 fluorescence microscope using an Olympus DP71 CCD camera (Olympus, Center Valley, PA). Micrographs were taken at a total magnification of 200× on the 4′, 6-diamidino-2-phenylindole dihydrochloride and fluorescein isothiocyanate fluorescence channels. All micrographs were taken at the same exposure conditions for accurate comparison. Images using both filters were overlaid to detect GFP expression.

Statistical analysis

Statistical significance between groups in the recellularized dermis model was determined using an unpaired *t*-test. Results are expressed as the mean ± standard error of the mean. Significant results were determined with respect to injection only controls. A *P* value less than 0.05 was considered significant.

Statistical significance between the groups for the murine model was determined by one-way analysis of variance with Student-Newman-Keuls multiple comparisons test (GraphPad Software, La Jolla, CA). Results are expressed as the mean ± standard error of the mean. Significant results were determined with respect to injection only controls. A *P* value less than 0.05 was considered significant.

CONFLICT OF INTEREST

The authors declared no conflict of interest.

ACKNOWLEDGMENTS

The authors thank Gary Walters of LifeNet Health, Virginia Beach, VA for gifting DermACELL® human allograft tissue with research consent.

REFERENCES

1. Goldston, RJ and Rutherford, PH. *Introduction to Plasma Physics*. Vol. 1. CRC Press, Boca Raton, 1995.
2. Hippler, R, Pfau, S, Schmidt, M and Schoenbach, KH. *Low Temperature Plasma Physics: Fundamental Aspects and Applications*. Rainer Hippler, Sigismund Pfau, Martin Schmidt, Karl H. Schoenbach (eds.). pp. 530. Wiley-VCH: Weinheim, Germany, 2001.
3. Napartovich, A (2001). Overview of atmospheric pressure discharges producing nonthermal plasma. *Plasmas and Polymers* **6**: 1–14.
4. Ermolaeva, SA, Sysolyatina, EV, Kolkova, NI, Bortsov, P, Tuhvatulin, AI, Vasiliev, MM *et al.* (2012). Non-thermal argon plasma is bactericidal for the intracellular bacterial pathogen Chlamydia trachomatis. *J Med Microbiol* **61**(Pt 6): 793–799.
5. Yu, Q, Huang, C, Hsieh, F-H, Huff, H and Duan, Y (2006). Sterilization effects of atmospheric cold plasma brush. *Applied Physics Letters* **88**: 013903-013903-3.
6. Zhang, Q, Sun, P, Feng, H, Wang, R, Liang, Y, Zhu, W, *et al.* (2012). Assessment of the roles of various inactivation agents in an argon-based direct current atmospheric pressure cold plasma jet. *J Appl Physics* **111**: 123305-123305-6.
7. Ardhaoui, M, Zheng, M, Pulpytel, J, Dowling, D, Jolivalt, C and Khonsari, FA (2013). Plasma functionalized carbon electrode for laccase-catalyzed oxygen reduction by direct electron transfer. *Bioelectrochemistry* **91**: 52–61.
8. Han, L, Lu, H, Patil, S, Keener, KM, Cullen, PJ and Bourke, P (2014). Bacterial inactivation by high-voltage atmospheric cold plasma: influence of process parameters and effects on cell leakage and DNA. *J Appl Microbiol* **116**: 784–794.
9. Heller, LC, Edelblute, CM, Mattson, AM, Hao, X and Kolb, JF (2012). Inactivation of bacterial opportunistic skin pathogens by nonthermal DC-operated afterglow atmospheric plasma. *Lett Appl Microbiol* **54**: 126–132.
10. Edelblute, CM, Malik, MA and Heller, LC (2015). Surface-dependent inactivation of model microorganisms with shielded sliding plasma discharges and applied air flow. *Bioelectrochemistry* **103**: 22–27.
11. Kong, MG, Kroesen, G, Morfill, G, Nosenko, T, Shimizu, T, Van Dijk, J, *et al.* (2009). Plasma medicine: an introductory review. *New Journal of Physics* **11**: 115012.
12. Fridman, G, Friedman, G, Gutsol, A, Shekhter, AB, Vasilets, VN and Fridman, A (2008). Applied plasma medicine. *Plasma Processes and Polymers* **5**: 503–533.
13. Daeschlein, G, Scholz, S, Ahmed, R, von Woedtke, T, Haase, H, Niggemeier, M *et al.* (2012). Skin decontamination by low-temperature atmospheric pressure plasma jet and dielectric barrier discharge plasma. *J Hosp Infect* **81**: 177–183.
14. Kelly-Wintenberg, K, Montie, TC, Brickman, C, Roth, JR, Carr, AK, Sorge, K *et al.* (1998). Room temperature sterilization of surfaces and fabrics with a one atmosphere uniform glow discharge plasma. *J Ind Microbiol Biotechnol* **20**: 69–74.
15. Liang, Y, Wu, Y, Sun, K, Chen, Q, Shen, F, Zhang, J *et al.* (2012). Rapid inactivation of biological species in the air using atmospheric pressure nonthermal plasma. *Environ Sci Technol* **46**: 3360–3368.
16. Jiang, C, Chen, M-T, Schaudinn, C, Gorur, A, Vernier, PT, Costerton, JW, *et al.* (2009). Pulsed atmospheric-pressure cold plasma for endodontic disinfection. *IEEE Trans Plasma Sci* **37**: 1190–1195.
17. Pan, J, Sun, P, Tian, Y, Zhou, H, Wu, H, Bai, N, *et al.* (2010). A novel method of tooth whitening using cold plasma microjet driven by direct current in atmospheric-pressure air. *IEEE Trans Plasma Sci* **38**: 3143–3151.
18. Kuo, S, Tarasenko, O, Chang, J, Popovic, S, Chen, C, Fan, H, *et al.* (2009). Contribution of a portable air plasma torch to rapid blood coagulation as a method of preventing bleeding. *New Journal of Physics* **11**: 115016.
19. Heinlin, J, Isbary, G, Stolz, W, Morfill, G, Landthaler, M, Shimizu, T, *et al.* (2011). Plasma applications in medicine with a special focus on dermatology. *J European Academy of Dermatology and Venereology* **25**: 1–11.
20. Weltmann, K, Brandenburg, R, Von Woedtke, T, Ehlbeck, J, Foest, R, Stieber, M, *et al.* (2008). Antimicrobial treatment of heat sensitive products by miniaturized atmospheric pressure plasma jets (APPJs). *Journal of Physics D: Applied Physics* **41**: 194008.
21. Gehl, J (2008). Electroporation for drug and gene delivery in the clinic: doctors go electric. *Methods Mol Biol* **423**: 351–359.
22. Heller, LC and Heller, R (2010). Electroporation gene therapy preclinical and clinical trials for melanoma. *Curr Gene Ther* **10**: 312–317.
23. Heller, R, Jaroszeski, MJ, Reintgen, DS, Puleo, CA, DeConti, RC, Gilbert, RA *et al.* (1998). Treatment of cutaneous and subcutaneous tumors with electrochemotherapy using intralesional bleomycin. *Cancer* **83**: 148–157.
24. Lucas, ML and Heller, R (2003). IL-12 gene therapy using an electrically mediated nonviral approach reduces metastatic growth of melanoma. *DNA Cell Biol* **22**: 755–763.
25. Miklavcic, D, Mir, LM and Thomas Vernier, P (2010). Electroporation-based technologies and treatments. *J Membr Biol* **236**: 1–2.
26. Mir, LM (2008). Application of electroporation gene therapy: past, current, and future. *Methods Mol Biol* **423**: 3–17.
27. Smith, AH, Fujii, H, Kuliszewski, MA and Leong-Poi, H (2011). Contrast ultrasound and targeted microbubbles: diagnostic and therapeutic applications for angiogenesis. *J Cardiovasc Transl Res* **4**: 404–415.
28. Gao, M, Ma, Y, Cui, R and Liu, D (2014). Hydrodynamic delivery of FGF21 gene alleviates obesity and fatty liver in mice fed a high-fat diet. *J Control Release* **18**: 1–11.
29. Liu, F and Huang, L (2002). Noninvasive gene delivery to the liver by mechanical massage. *Hepatology* **35**: 1314–1319.
30. Liu, F, Lei, J, Vollmer, R and Huang, L (2004). Mechanism of liver gene transfer by mechanical massage. *Mol Ther* **9**: 452–457.
31. Daud, AI, DeConti, RC, Andrews, S, Urbas, P, Riker, AI, Sondak, VK *et al.* (2008). Phase I trial of interleukin-12 plasmid electroporation in patients with metastatic melanoma. *J Clin Oncol* **26**: 5896–5903.
32. Wang, W, Li, W, Ma, N and Steinhoff, G (2013). Non-viral gene delivery methods. *Curr Pharm Biotechnol* **14**: 46–60.
33. Schoenbach, KH and Malik, MA (2014). Scaling of shielded sliding discharges for environmental applications. *Plasma Chemistry and Plasma Processing* **34**: 39–54.
34. Malik, MA, Xiao, S and Schoenbach, KH (2012). Scaling of surface-plasma reactors with a significantly increased energy density for NO conversion. *J Hazard Mater* **209-210**: 293–298.
35. Malik, MA and Schoenbach, KH (2012). New approach for sustaining energetic, efficient and scalable non-equilibrium plasma in water vapours at atmospheric pressure. *Journal of Physics D: Applied Physics* **45**: 132001.
36. Connolly, RJ, Lopez, GA, Hoff, AM and Jaroszeski, MJ (2010). Characterization of plasma mediated molecular delivery to cells *in vitro*. *Int J Pharm* **389**: 53–57.
37. Connolly, RJ, Lopez, GA, Hoff, AM and Jaroszeski, MJ (2009). Plasma facilitated delivery of DNA to skin. *Biotechnol Bioeng* **104**: 1034–1040.
38. Connolly, RJ, Rey, JI, Lambert, VM, Wegerif, G, Jaroszeski, MJ and Ugen, KE (2011). Enhancement of antigen specific humoral immune responses after delivery of a DNA plasmid based vaccine through a contact-independent helium plasma. *Vaccine* **29**: 6781–6784.
39. Shah, K, Connolly, RJ, Chapman, T, Jaroszeski, MJ and Ugen, KE (2012). Electrogenetherapy of B16.F10 murine melanoma tumors with an interleukin-28 expressing DNA plasmid. *Hum Vaccin Immunother* **8**: 1722–1728.
40. Edelblute, CM, Heller, LC, Malik, MA and Heller, R (2015). Activated air produced by shielded sliding discharge plasma mediates plasmid DNA delivery to mammalian cells. *Biotechnol Bioeng* **112**: 2583–2590.
41. Schoop, VM, Mirancea, N and Fusenig, NE (1999). Epidermal organization and differentiation of HaCaT keratinocytes in organotypic coculture with human dermal fibroblasts. *J Invest Dermatol* **112**: 343–353.
42. Dobrynin, D, Fridman, G, Friedman, G and Fridman, A (2009). Physical and biological mechanisms of direct plasma interaction with living tissue. *New J Physics* **11**: 115020.
43. Kim, JG, Yousef, AE and Dave, S (1999). Application of ozone for enhancing the microbiological safety and quality of foods: a review. *J Food Prot* **62**: 1071–1087.
44. Choi, JH, Nam, SH, Song, YS, Lee, HW, Lee, HJ, Song, K *et al.* (2014). Treatment with low-temperature atmospheric pressure plasma enhances cutaneous delivery of epidermal growth factor by regulating E-cadherin-mediated cell junctions. *Arch Dermatol Res* **306**: 635–643.
45. Pouvesle, J-M, Collet, G, Robert, E, Ridou, L, Brullé, L, Ries, D, *et al. Potential of plasma based soft and/or combined cancer treatments, in 22nd International Symposium on Plasma Chemistry*. 2015: Antwerp, Belgium.
46. Darny, T, Robert, E, Pechereau, F, Dozias, S, Bourdon, A and Pouvesle, J-M. *2D time-resolved measurement and modeling of electric fields associated with atmospheric pressure plasma streams propagation in dielectric capillaries, in 22nd International Symposium on Plasma Chemistry*. 2015: Antwerp, Belgium.
47. Mendis, DA, Rosenberg, M and Azam, F (2000). A note on the possible electrostatic disruption of bacteria. *Ieee Transactions on Plasma Science* **28**: 1304–1306.
48. Heller, LC, Jaroszeski, MJ, Coppola, D, McCray, AN, Hickey, J and Heller, R (2007). Optimization of cutaneous electrically mediated plasmid DNA delivery using novel electrode. *Gene Ther* **14**: 275–280.
49. Heller, LC and Heller, R (2006). *In vivo* electroporation for gene therapy. *Hum Gene Ther* **17**: 890–897.
50. Connolly, RJ, Hoff, AM, Gilbert, R and Jaroszeski, MJ (2015). Optimization of a plasma facilitated DNA delivery method. *Bioelectrochemistry* **103**: 15–21.
51. Bulysheva, AA, Burcus, N, Lundberg, C, Edelblute, CM, Francis, MP and Heller, R (2016). Recellularized human dermis for testing gene electro transfer *ex vivo*. *Biomed. Mater* (in press).